Fabrication of an antireflective polymer optical film with subwavelength structures using a roll-to-roll micro-replication process

2008 J. Micromech. Microeng. 18 075001

(http://iopscience.iop.org/0960-1317/18/7/075001)

IOP PUBLISHING JOURNAL OF MICROMECHANICS AND MICROENGINEERING

J. Micromech. Microeng. **18** (2008) 075001 (9pp) doi:10.1088/0960-1317/18/7/075001

Fabrication of an antireflective polymer optical film with subwavelength structures using a roll-to-roll micro-replication process

Chia-Jen Ting[1,2], Fuh-Yu Chang[2], Chi-Feng Chen[3] and C P Chou[1]

[1] Mechanical Engineering Department, National Chiao Tung University, Taiwan 300, Republic of China
[2] Mechanical and Systems Research Laboratories, Industrial Technology Research Institute, Taiwan 310, Republic of China
[3] Department of Mechanical Engineering/Institute of Opto-Mechatronics Engineering, National Central University, Chung-li, Taiwan, Republic of China

E-mail: ccf@cc.ncu.edu.tw

Received 26 November 2007, in final form 14 March 2008
Published 20 May 2008
Online at stacks.iop.org/JMM/18/075001

Abstract

An antireflective optical film with subwavelength structures replicated by use of a roll-to-roll micro-replication process (RMRP) is investigated. Firstly, a single layer of a nanostructure on a polymer film is designed for an antireflection purpose by the finite difference time domain method in the visible light spectrum. Structures of a conical cylinder array, with spatial period of 400 nm, diameter of 200 nm and height of 350 nm, are numerically obtained. Then, such structures are fabricated by RMRP combining originated structure fabrication realized by deep ultra-violet lithography and dry etching, Ni mold electroplating and replication by using the roll-to-roll process imprinting into the flexible polyethylene terephthalate substrate. A nanostructure roller mold bonded with Ni molds has been successfully fabricated and coated with the self-assembly monolayer process for the purpose of fabricating an anti-adhesion film and improving the lifetime of the Ni molds. The duplicated nanostructure films show a good optical quality of antireflection (AR $\leqslant$ 2.45% in a 400–700 nm spectral range) and are in good agreement with the theoretical predictions. The experimental results show that the developed process is a promising and cost-effective method for the continuous duplication of flexible devices with nano-scaled feature sizes used in nanophotonics by RMRP.

(Some figures in this article are in colour only in the electronic version)

1. Introduction

Due to the fast development in computer-aided design and micro/nano-fabrication technologies, optical elements with functional subwavelength structures have been successfully implemented in light emitting diodes [1], photo detectors [2], solar systems [3–6], displays [6, 7], glass components [8, 9] and so on. The designed two-dimensional (2D) subwavelength structures on an element surface can suppress Fresnel reflection. Such structures are called antireflection subwavelength structures (ASSs). Well-known ASSs, called moth eye structures, were first discovered on the cornea of night-flying moths [10]; prominences on the moth eye are structures, antireflective in nature. Recently they have been proposed as applicable alternatives, based on both theoretical and experimental studies [11–14]. Under a zero reflectivity target, the functional dependences of the reflectivity on the filling factor, groove depth, angle of incidence and polarization for rectangular-groove high spatial-frequency dielectric gratings are calculated using rigorous coupled-wave analysis [11]. The gratings are shown to be capable of exhibiting zero reflectivity. An antireflection surface

in Si is designed by rigorous coupled-wave analysis and fabricated by using binary optics technology [12]. In a long-wavelength infrared region, the results show that transmittance significantly increases. Fabrication of 2D ASSs in the visible spectral range has been reported for semiconductor materials [13]. Then, the surface of a 2D ASS upon a crystal Si substrate was fabricated by electron beam lithography and etched by an SF_6 fast atom beam [14]. A conical profile structure is shown, the period is 150 nm and the groove is approximately 350 nm deep.

Fresnel reflection will lead to some disadvantages for many optical systems, such as reducing the share of transmitted light, deteriorating the contrast of displays and generating the formation of ghost images in imaging systems, and so needs to be omitted or suppressed. Especially, portable electronics, such as a laptop computer, digital camera, camcorder, mobile phone and PDA, are frequently used in outdoor or under high brightness circumstances. Generally, it is reduced by the use of antireflection coating technology [15, 16]. Although coating technology is maturely used on different surfaces, it still has problems associated with limitations in the coating materials and various physical and chemical properties that will affect adhesion, thermal mismatch and the stability of the thin-film stack [14, 17]. Therefore, developing a cost-effective and efficient fabrication technology to fabricate an optical element with antireflection structures is becoming critical and in great demand.

A micro-replication process (MRP), combining originated micro/nano-structure fabrication, metallic mold electroplating and replication into plastics, offers a high-speed method to produce low-cost components and modules with micro/nano-structures [5–7, 18–20]. Generally, the originated structure pattern is designed by one of the optical design programs [11, 12, 18]. The designed structure pattern is realized by several approaches, such as interference lithography [6, 21], gray-scale lithography [22], photolithography [23] and ultra-precision machining [24]. The materials of these templates are not important since the next step is metallic mold electroplating. For the step of replication into plastics, technologies, mainly injection molding [25], hot embossing [26], UV embossing [6, 27], injection compression molding and thermoforming [28], are available for reproducing high-resolution micro-structure and nano-structure features in plastics from a high-resolution mold. MRP has been widely studied and applied to fabricate the polymer optical elements. For example, optical components in solar and display applications are replicated by interference lithography micro-replication techniques [6]; a polarizer formed as a metal wire grid with periodicity in the 200–400 nm regime is fabricated using a replication process with slope metal evaporation technology to replace a more costly high-resolution lithography and etching process [29]; a polymeric diffractive microlens for coupling the incident light to two individually plastic optical fibers is designed and fabricated by a UV imprinting process. The diffractive microlens structure, whose pixel width is 1 μm, is successfully duplicated on a polyethylene terephthalate (PET) substrate and the measurement results of optical properties are excellent [27]. The replicated elements having advantages of a precise profile, low costs and light weight are highly suited for the demands of the optical industry and are expected to play a major role in the production of optical microsystems and micro-optical elements.

For the cost-effective fabrication of large area products, roll-to-roll manufacturing is always an ideal method. Typical product examples are newspapers and labels. Recently, it is also applied in high-tech products such as organic light emitting diodes (OLED), thin film solar cells, optical brightness enhancement films or organic thin film transistors (OFET) [19, 30–36]. As such, roll-to-roll (R2R) enters into the micro-replication process, called a roll-to-roll micro-replication process (RMRP), can be most available and powerful for the continuous production of a large area, is low cost and has high-resolution optical films with a micro/nano-structure for different purposes at room temperature [19, 34–36]. A representative product is Vikuiti^{TM} brightness enhancement films (BEF) which can increase the LCD brightness through improved management of the existing light. Typical BEF II is a microreplicated prismatic structured film, with a prism peak angle of 90° and a prism peak spacing of 50 mm[4]. When optical films with submicro-structures, even nano-structures, produced by RMRP come true, it will provide unprecedented throughput for many practical applications [37].

In this study, we design and fabricate periodic conical ASSs upon a flexible PET substrate. The fabricated ASSs are designed by the finite difference time domain (FDTD) method. The periodic conical cylinder structured surface is fabricated by RMRP combining originated structure fabrication realized by deep ultra-violent (DUV) lithography and dry etching, Ni mold electroplating and replication by using the R2R process imprinting into the flexible PET substrate. The optical property of the fabricated film shows good agreement with the simulation results.

2. Simulation method and results

The FDTD method is an accurate and available technique to study the antireflection effect of the surface with an ASS. In this study, the FDTD method is used to design the parameters of the periodic conical shape with an antireflection function in the 400–700 nm spectral range. To meet the aim and consider the replication technology, a 2D periodic array of a subwavelength cylinder combined a half of an ellipsoid as a simulation geometric mold; the schematic profile can be seen in figure 1. Figure 1 shows the schematic profile of the ASS onto the polymer material surface. Here, p is the spatial period, h is the structure height, b is the radius of the ellipsoid in the Z-direction and a is the diameter of the ellipsoid in the X- or the Y-direction. n_0 and n_s are the refractive indices of the incident medium and polymer material, respectively. Here, we choose $n_0 \approx 1.00$ for air and $n_s = 1.54$. We consider a light-wave propagating from the air through the ASS surface into the polymer material and ignore the absorption loss of the medium. On the other hand, since the FDTD

[4] http://www.mmm.com, Vikuiti^{TM} Display Enhancement Films, 3M company, USA.

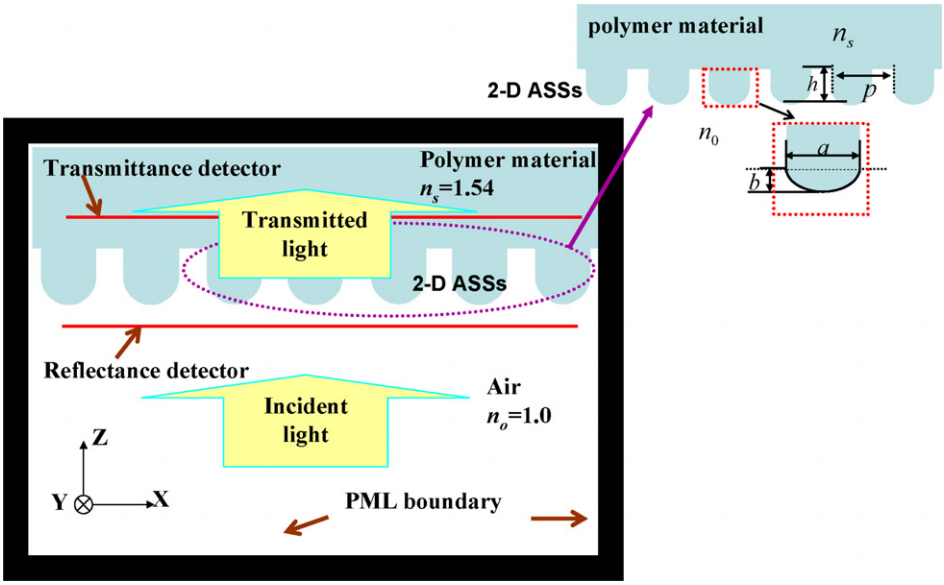

Figure 1. Sketch of the light-wave propagation through an optical film with a 2D ASS simulated by the FDTD method.

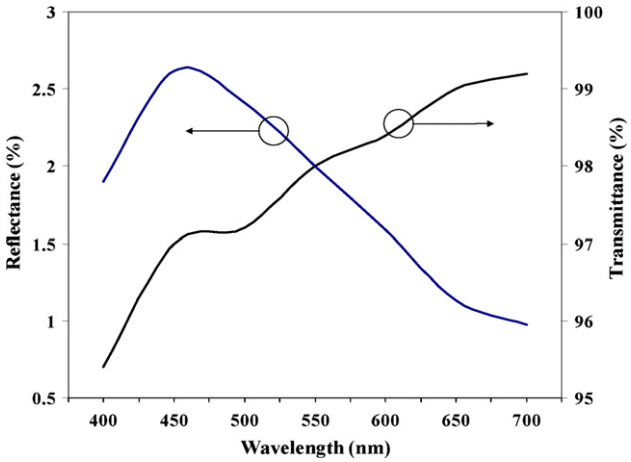

Figure 2. Variances of the simulation values of reflectance and transmittance.

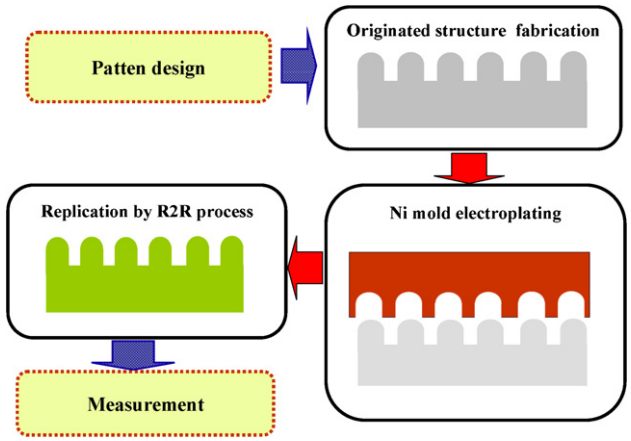

Figure 3. Schematic illustration of RMRP.

has finite analysis windows, an artificial boundary condition suppressing reflections at the analysis windows is required. In the FDTD simulation, absorbing boundary conditions are needed to truncate the computation domain without reflection. To decrease the error induced by the boundary of the simulated area, a perfect matched layer (PML) is applied [38]. The dispersion effect, which describes the dependence of the refractive index of the medium on frequency, is ignored in this material.

By the FDTD method, the parameters of the ASS surface are the spatial period $p = 400$ nm, the structure height $h = 350$ nm, $a = 100$ nm and $b = 200$ nm. The variances of the simulation values of reflectance and transmittance in the 400–700 nm range are shown in figure 2. It is seen that these reflectance and transmittance results are larger than 96% and smaller than 2.6%, respectively. The average simulated reflectance and transmittance are about 97.6% and 1.87%, respectively.

3. Fabrication process, results and discussion

In this study, we use RMRP to fabricate the optical element with the simulated nanostructures. The schematic illustration of RMRP is shown in figure 3. First, the originated nanostructures are fabricated on a Si wafer as the master. The Si master is then transferred onto a Ni mold by micro-electroplating. Finally, with this precision mold, the structures are replicated onto the flexible PET substrate by using the roll-to-roll process. Next, we will describe the above process in detail.

3.1. Originated structure fabrication: DUV lithography and dry etching

In the present work, we use an 8-inch P-type (1 0 0) Si wafer as a substrate. It is firstly cleaned by acetone and isopropyl alcohol. The high-resolution photoresist (Shin-Etsu YSB663) of 230 nm thickness is spun on the wafer by a spin

Table 1. Composition of the chemical solution and operating parameters used in an electroless plating process.

Electroless solution		Sensitization solution		Activation solution	
Composition	Unit (g L^{-1})	Composition	Unit	Composition	Unit
$NiSO_4 \cdot 6H_2O$	20	$SnC_{l2} \cdot 2H_2O$	100 g L^{-1}	$PdCl_2$	0.5 g L^{-1}
$Na_2C_4H_4O_4$	16	HCl (35%)	70 mL L^{-1}	HCl (35%)	2mL L^{-1}
$NaH_2PO_2 \cdot H_2O$	27			Working temperature	40 °C
Pb^{+2}	0.54 ppm				
PH	4.8				
Solution temperature	80 ± 1 °C				

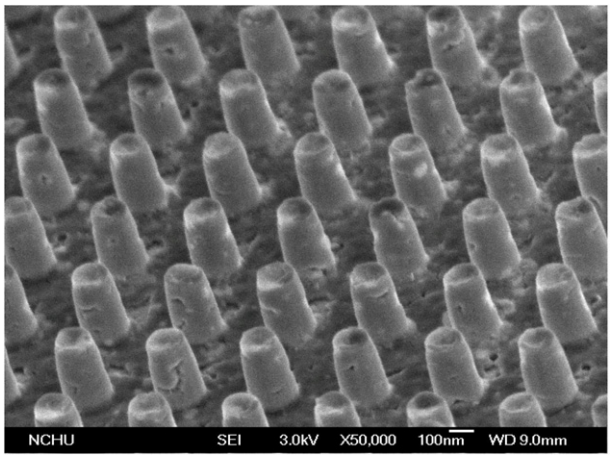

Figure 4. SEM image of a 2D cylinder array on the Ni mold.

coater. Patterning is carried out by an 8-inch stepper (Nikon NSR2250EX-12B) and a developer.

The developed wafer is treated with a dry etching process to transfer the patterns of photoresist into the Si substrate by an ICP-RIE system (Oxford ICP S100). Etching conditions are tuned under using different combinations of SF_6, O_2 and C_4F_8 gases, and the working pressure is maintained at 6 m Torr. After removing the residual photoresist, the originated nanostructure template of the Si substrate, called the Si master, is finished.

3.2. Ni mold electroplating

For the flexible Ni mold, electroless plating is used to transfer the nanostructures with the originated structures (etched Si master). Electroless plating is a chemical reaction to make the metal ion react on the surface of the target. We firstly put the active nuclei of metal, Pd, on the surface of target by the sensitization process and then emerge it in DI water at 70 °C for preheating. The electroless plating process is carried out in the PTFE tank, produced by the Industrial Technology Research Institute (ITRI), with a chemical solution at elevated temperature. Table 1 shows the composition of the solution and operating parameters. The final thickness of the nanostructure Ni mold is according to the deposition time, and the normal thickness of the Ni mold in this study varies from 50 to 200 μm. The plated Ni mold is cleaned by DI water and then dried by nitrogen. The template has been further heat treated in a nitrogen atmosphere to release the residual stress and hydrogen atom, which are the key issues

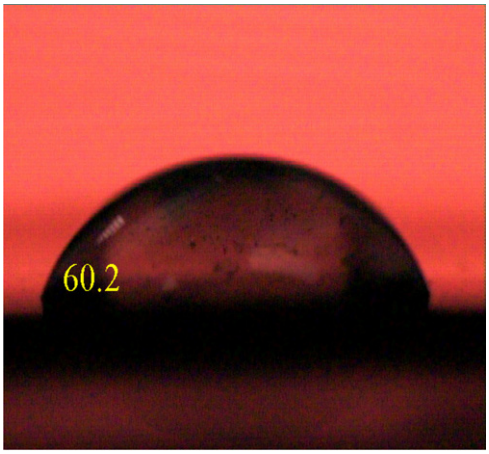

(*a*)

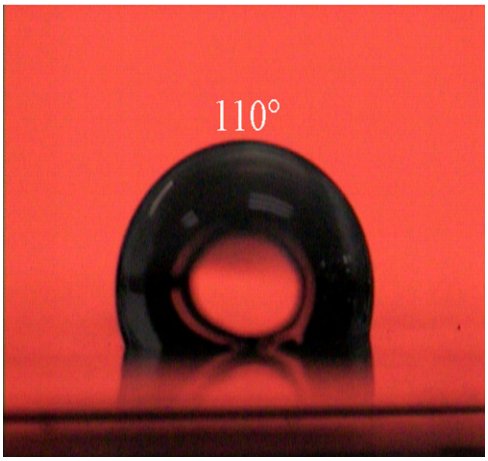

(*b*)

Figure 5. Contact angle measurements of the Ni mold before (*a*) and after (*b*) the SAM deposition.

inducing the warp and hydrogen brittleness of the template. Figure 4 shows a SEM image of the 2D cylinder array on the Ni mold duplicated from a patterned Si master.

To decrease the surface energy of Si and Ni molds and meet the requirement of anti-stick in the imprinting process, self-assembly monolayer (SAM) deposition in a vacuum chamber is adapted or surface treatment of Si and Ni molds. The SAM material used in this study is 1H, 1H, 2H, 2H–perfluorooctyltrichorosilane. To maintain the water-free atmosphere, a newly designed vacuum chamber system has been designed to deposit the SAM molecule. The Si stamps are firstly cleaned by acetone, and then dipped in the solution

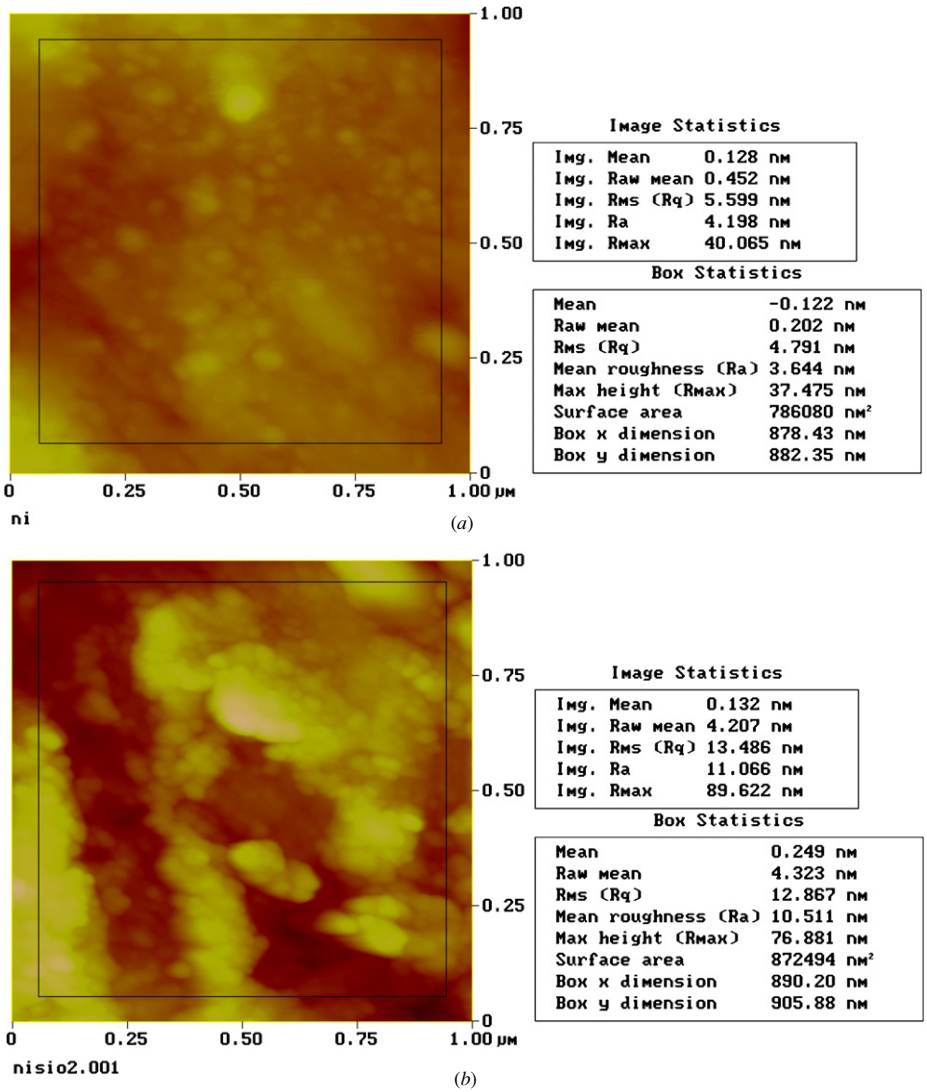

Figure 6. Roughness analysis of the Ni mold by using AFM without (*a*) and with (*b*) the SiO_x buffer layer of 20 nm.

of hydrogen peroxide and sulfuric acid (1:3, vol.%) for 10 min to remove the metal and organic contamination on the surface. The cleaned Si is soon put into a solution of 70% nitric acid to form O–H bonding on the surface and cleaned again with DI water and dried with pure nitrogen gas. On the other hand, the Ni mold is treated by an oxygen plasma for about 10 min soon after cleaning with acetone. A nanoscaled oxide film (NiO_x) has been grown on the surface in this step. To keep the water content as low as possible in the deposition process of SAM, a simple vacuum chamber, integrated with a heating system, is used. Before each deposition process begins, the chamber is evacuated to about 2×10^{-3} Torr and then pure nitrogen gas is poured into it. The process is repeated for at least three times to keep the water content in the chamber less than 1 ppm. The stamp in the chamber is then heated to about 150 °C to remove the water and other molecules adhered to the surface. The vacuum gate is closed when the vaporized molecules of SAM flow into the chamber by a vacuum effect. The deposition pressure and time are maintained at about 20–25 Torr and 5 min, respectively. The coated stamp is cleaned in the solution of acetone to prevent the residual molecules on the stamp reacting with the water in the atmosphere. It is well known that a stamp possesses a good anti-adhesive property if the stamp has a very low surface energy. For surface analysis related to surface energy and tension, the measurement of the contact angle which is the angle at which a liquid/vapor interface meets the solid surface is usually adopted as a simple method[5].

The SAM-treated stamp is characterized by contact angle measurement equipment before and after imprint processes. Figures 5(*a*) and (*b*) show the contact angles of 60.2° and 110°, respectively, of the Ni mold before and after the SAM deposition. The template surfaces are changed from hydrophilic to hydrophobic in nature. It also indicates that the surface energy of the Ni stamps has been strongly lowered by the SAM deposition.

[5] http://en.wikipedia.org/wiki/Contact_angle.

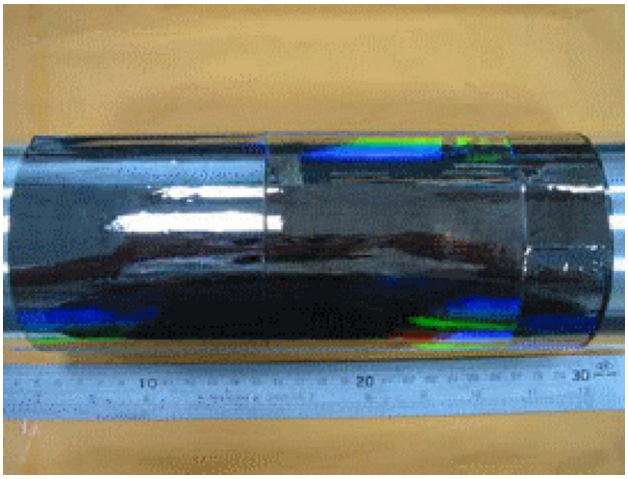

Figure 7. Picture of the bonded roller mold adhered with the ASS Ni mold.

To further improve the quality of the SAM coating, SiO_x and TiO_x thin films are used for buffer layers on the Ni mold. The condition of the buffer layer treatment is as follows. (1) SiO_x film: pre-O_2 plasma for 5 min, then ion beam sputtering for 10 min; (2) TiO_x film: pre-O_2 plasma for 5 min, ion beam sputtering for 5 min, then additional O_2 plasma for 5 min. The beam voltage of the sputter is kept at 500 V and the current is 130 mA. The thicknesses of buffer layers SiO_x and TiO_x are 20 nm and 12 nm, respectively. Figure 6 shows roughness analysis of the Ni mold by using AFM without (a) and with (b) the SiO_x buffer layer of 20 nm. One can see that the roughness of the Ni mold before and after SiO_x coating is Ra 3.4 nm and Ra 10.5 nm, respectively.

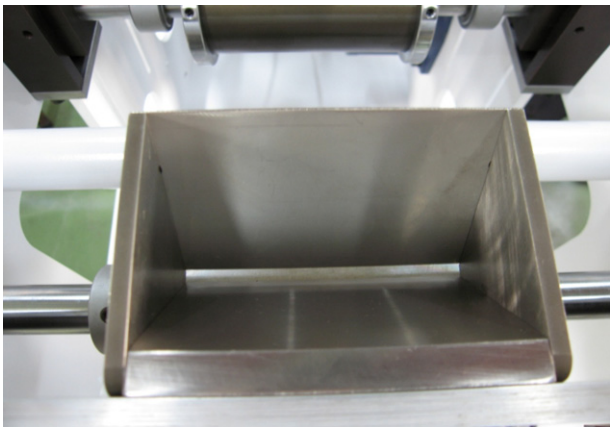

Figure 9. Picture of the high precision knife-type UV resin distributor, designed by ITRI.

3.3. Replication by using the R2R imprinting process

The nanostructure Ni molds treated by SAM deposition are bonded to the roller mold with a magnetic film to make the nanostructure roller mold for the R2R imprinting process. The bonded nanostructure roller mold is shown in figure 7. The bonded roller mold is 20 cm in diameter. The roller mold is set up in MSL-50A R2R nanoimprinting equipment produced by ITRI and shown in figure 8. The UV light source, used a bar bulb (Philips, 400 W, $\lambda = 365$ nm) with a self-designed light box to guide the UV light uniformly to the cylindrical mold, is used for curing resin in this equipment. UV curable resin (Mitsubishi 7700) is distributed on the PET substrate by a resin distributor of the knife type, as shown in figure 9, and the thickness of the coated resin can be adjusted from 50 to 200 μm with 10% variation. The parameters of UV curable

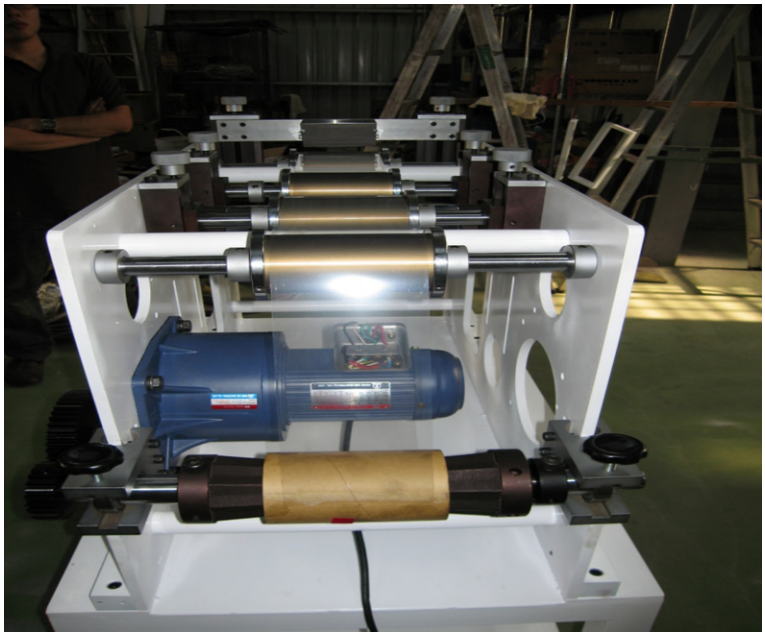

Figure 8. Picture of the R2R imprinting equipment, MSL-50A designed by ITRI, for continuous nanostructure duplication.

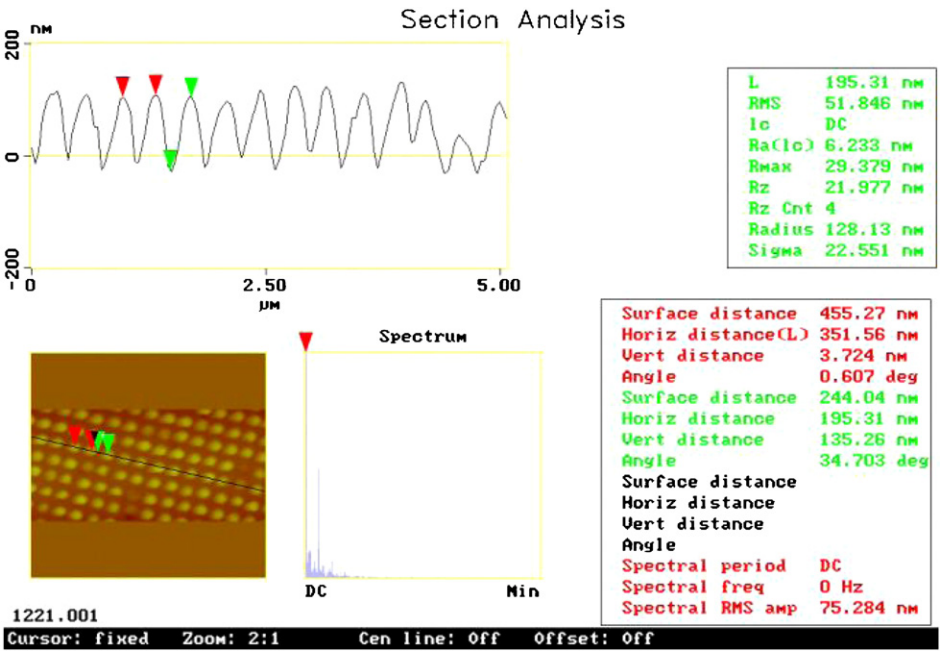

Figure 10. AFM image of the replication structures on the PET film.

resin parameters are refractive index 1.54, viscosity 400 cps and UV curing exposure energy 400 mJ cm^{-2}.

In this study, the rolling speed ranges from 2 to 5 m min^{-1}. The PET film of 0.2 mm in thickness (Mitsubishi A4100#125) is used as the substrate in the experiments. The exposure intensity is 91 mW cm^{-2}. The sample is exposed to a curing system for about 5–10 s; the resin is solidified at room temperature.

3.4. Results and discussion

Figure 10 shows an AFM image of the replication structure on the PET film. One can see the duplicated structure with the same feature size of the roller mold, except for the lower structure height. The effective width of the replicated element can be up to about 280 mm. A picture of a large area sample, with a diagonal size of about 400 mm, is shown in figure 11. The antireflective effect of the duplicated nano-structure is found in this picture.

It is caused by insufficient filling of UV resin into the mold structure. It can be improved by increasing the surface tension of the substrate or adding vertical pressure to the backside of the flexible substrate. There are still other ways to improve the duplication of geometry, such as preheating of the substrate and modification of UV resin. On the other hand, to improve the surface condition for easy filling, demolding is another alternative.

In addition, to understand the effect of the Ni mold with SAM, UV-imprint processes have been executed several hundred times. Figure 12 show SEM images of the nanostructure templates after hundreds of nanoimprinting processes without (a) and with (b) SAM treatment. It is seen from figure 12(*a*) that, when the template is not coated with the SAM, parts of the duplicated nanostructure may fracture during the demolding procedure. When the Ni templates with SAM deposition have been used for imprinting hundreds of times, the duplicated structures are almost the same as the very first duplicated nanostructures. Moreover, no stains of polymeric residue or parts of the fractured nanostructure have been found on the Ni mold with SAM. This means that the SAM adhered very well to the template surface in this study. Also, the SAM can strongly improve the lifetime of the Ni molds.

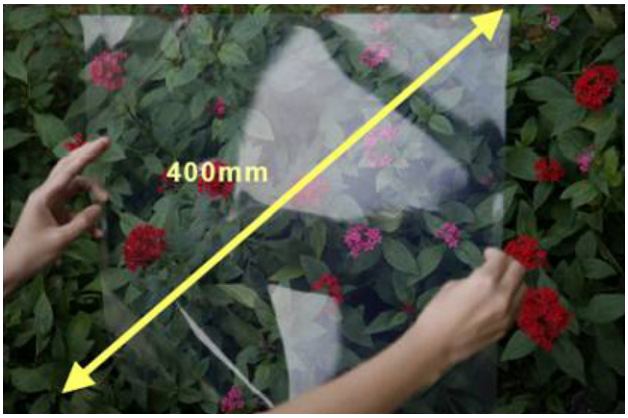

Figure 11. Picture of a large area replicated element.

4. Optical property of measurement results and discussions

The spectroscopic measurement is measured in the reflectance of the replicated prototype using a MODELV-570 spectrometer supplied by JASCO International Co., Ltd. The measured

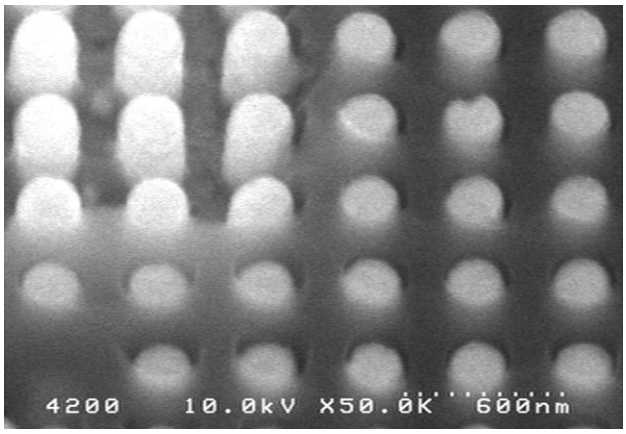

(*a*)

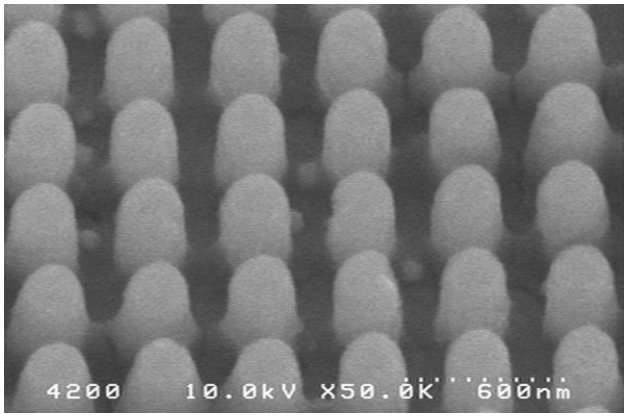

(*b*)

Figure 12. SEM images of the nanostructure templates after hundreds of nanoimprinting processes without (*a*) and with (*b*) SAM treatment.

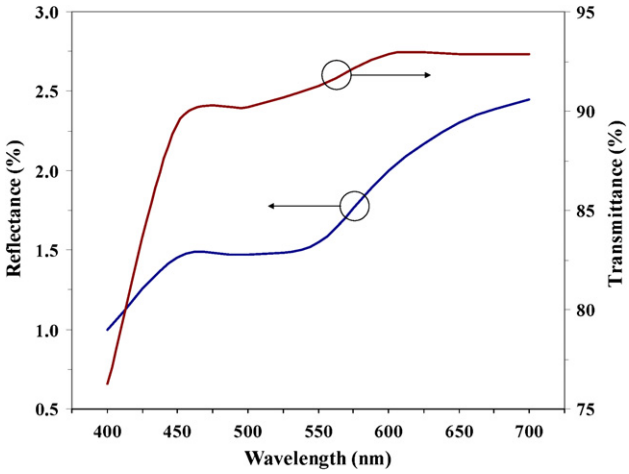

Figure 13. Variances of the measured values of reflectance and transmittance.

results of the reflectance and transmittance of the flexible PET film with ASSs are shown in figure 13. In 400–700 nm spectral ranges, the reflectances of the replicated prototype are below 2.45% and the average one is about 1.75%. Comparing experiment and simulation results, the average difference value is about 0.54%. The transmittances of the replicated prototype are above 89.4% and the average one is about 91.6% in the 450–700 nm spectrum range. When the light propagates from the air into the PET film (the refractive index ≈1.62) at the normal incidence and the dispersion effect is ignored, the theoretical reflectance result of this interface is about 5.60%. When the light is through the PET film, the theoretical transmittance result is close to 89.1%. Comparing the above results, the optical property of the fabricated film shows good agreement with the simulation result, except for the transmittance of the experiment result at wavelength 400 nm.

5. Conclusions

Antireflective optical film with subwavelength structures replicated by use of RMRP is investigated. The fabricated ASSs are designed by the FDTD method. Structures of a conical cylinder array, with spatial period of 400 nm, diameter of 200 nm and height of 350 nm, are obtained. It is shown that the average simulated reflectance and transmittance are about 97.6% and 1.87%, respectively. Then, the structures are fabricated by RMRP combining originated structure fabrication realized by DUV lithography and dry etching, Ni mold electroplating and replication by using R2R process imprinting into the flexible PET substrate. The nanostructure roller mold bonded with Ni molds has been successfully fabricated and coated with the SAM process for the purpose of fabricating an anti-adhesion film and improving the lifetime of the Ni molds. In 400–700 nm spectral ranges, the reflectances of the replicated prototype are below 2.45% and the average one is about 1.75%. The transmittances of the replicated prototype are above 89.4% and the average one is about 91.6% in the 450–700 nm spectrum range. The experimental results show that the developed process is a promising and cost-effective method for the continuous duplication of flexible devices with nano-scaled feature sizes used in nanophotonics by R2R nanoimprinting processes.

References

[1] Kanamori Y, Ishimori M and Hane K 2002 *IEEE Photon. Technol. Lett.* **14** 1064–6
[2] Ishimori M, Kanamori Y, Sasaki M and Hane K 2003 *Japan. J. Appl. Phys.* **41** 4346–9
[3] Kanamori Y, Kobayashi K, Yugami H and Hane K 2003 *Japan. J. Appl. Phys.* **42** 4020–3
[4] Heine C and Morf R H 1995 *Appl. Opt.* **34** 2476–82
[5] Gombert A *et al* 1998 *Sol. Energy Mater. Sol. Cells* **54** 333–42
[6] Gombert A *et al* 2004 *Opt. Eng.* **43** 2525
[7] Boerner V, Abbott S, Bläsi B, Gombert A and HoBfeld W 2003 *SID 03 Dig.* pp 68–71
[8] Kanamori Y, Kikuta H and Hane K 2000 *Japan. J. Appl. Phys.* **39** L735–7
[9] Kintaka K, Nishii J, Mizutani A, Kikuta H and Nakano H 2001 *Opt. Lett.* **26** 1642–4
[10] Bernhard C G 1967 *Endeavour* **26** 79–84
[11] Gaylord T K, Baird W E and Moharam M G 1986 *Appl. Opt.* **25** 209–14

[12] Motamedi M E, Southwell W H and Gunning W J 1992 *Appl. Opt.* **31** 225–9
[13] Lalanne P and Morris G M 1997 *Nanotechnology* **8** 53–6
[14] Kanamori Y, Sasaki M and Hane K 1999 *Opt. Lett.* **24** 1422–4
[15] MacLeod A 2001 *Thin-Film Optical Filters* 3rd edn (Bristol: Institute of Physics Publishing)
[16] Willey R 2002 *Practical Design and Production of Thin Films* (New York: Dekker)
[17] Lalanne P and Morris G M 1996 *Proc. SPIE* **2776** 300–9
[18] Sinzinger S and Jahns J *Microoptics* 2nd edn (Weinheim: Wiley-VCH)
[19] Gale M T *et al* 2005 *Opt. Lasers Eng.* **43** 373–86
[20] Heckele M and Schomburg W K 2004 *J. Micromech. Microeng.* **14** R1–14
[21] Wadle S, Wuest D, Cantalupo J and Lakes R S 1994 *Opt. Eng.* **31** 213–8
[22] Oppliger Y, Sixt P, Stauffer J M, Mayor J M, Regnault P and Voirin G 1994 *Microelectron. Eng.* **23** 449–54
[23] Swanson G J and Weldkamp W B 1987 High-efficiency, multi-level, diffractive optical elements *US Patent* 4895790
[24] Weck M, Fischer S and Vos M 1997 *Nanotechnology* **8** 145–48
[25] Hanemann T, Heckele M and Piotter V 2000 *Polym. News* **25** 224–9
[26] Heckele M, Bacher W and Müller K D 1998 *Microsyst. Technol.* **4** 122–4
[27] Yang J J, Chen C F and Liao Y S 2008 *Opt. Commun.* **28** 474–9
[28] Dreuth H and Heiden C 1999 *Sensors Actuators* A **78** 198–204
[29] Schnieper M, Di Prima F, Zschokke C, Gale M T and David C 2003 Fabrication and application of subwavelength gratings *Proc. Int. Conf. on Diffractive Optics DO 2003 (Oxford, UK, Sep.)* pp 16–22
[30] Izu M and Ellison T 2003 *Solar Energy Mater. Solar Cells* **78** 613–26
[31] Gale M T 2003 *Opt. Photon. News* **14** 24–9
[32] Jain K, Klosner M, Zemel M and Raghunandan S 2005 *Proc. IEEE* **93** 1500–10
[33] Bowden N, Brittain S, Evans A G, Hutchinson J W and Whitesides G M 1998 *Nature* **393** 146–9
[34] Tan H, Gilbertson A and Chou S Y 1998 *J. Vac. Sci. Technol.* B **16** 3926–8
[35] Mäkelä T, Haatainen T, Majander P and Ahopelto J 2007 *Microelectron. Eng.* **84** 877–9
[36] Mäkelä T, Haatainen T, Majander P and Ahopelto J 2005 *Trends in Nanotechnology 2005 (TNT 2005) (Oviedo, Spain, 29 Aug.–02 Sep.)*
[37] Guo L J 2007 *Adv. Mater.* **19** 495–513
[38] Berenger J P 1996 *IEEE Trans. Antennas Propag.* **44** 110–7